# The effect of heat treatment on the microstructural changes and hardness of cast $Ni_{50}Ti_{30}Zr_{20}$ alloy

*Paul* Shangase[1], *Charles* Siyasiya[1] and *Jelena* Skamat[2]

[1] Department of Materials Science and Metallurgical Engineering, University of Pretoria, South Africa
[2] Vilnius Gediminas Technical University, Institute of Building Materials Laboratory of Composite Materials, Lithuania

**Abstract.** The nickel-based shape memory alloys (SMAs) provide attractive properties *inter alia* lightweight and simple compact mechanical designs requiring low actuating force levels. However, there is a limit to their functional properties such as super-elasticity and shape memory effects, as they cannot perform well above 100°C. Thus, there is a need to improve these properties for applications of these alloys beyond their maximum transformation temperatures, by alloying them with elements like Zr. The aim of this study is to examine how heat treatments affect microstructural evolution is crucial for SMAs designed for high-temperature application. As microstructures are closely related to mechanical properties, analysis of the changes in mechanical properties through various heat treatment processes may provide key information on how to design alloys with superior mechanical properties. In order to create a homogeneous microstructure and eliminate chemical segregation, six samples (5 × 10 × 10 mm) were homogenised at 1000°C. Samples were then aged for one hour and three hours at heat treatment temperatures of 550°C, 750°C, and 800°C. The samples were analysed using SEM, XRD and Vickers hardness. The results show a microstructure with a $(Ti, Zr)_2Ni$ phase that precipitated due to heat treatment and resulted in increased hardness.

## 1 Introduction

The evolution of civilisation is intricately linked to advancements in materials science [1]. Humanity's continuous sustenance is dependent on the improvement of more technologically advanced developments [2]. In recent decades; advancements in materials research have been driven by the discovery of novel material properties [3]. Currently, shape memory alloys (SMAs) are widely utilised in various technical domains, including automotive [4, 5], aerospace [6-8] and medicine [9-12], where they serve well as actuators or connectors in electronic systems[12]. The most commonly known shape memory alloy is nickel-titanium commonly known as nitinol [13]. Nitinol is an alloy in which the two elements are present in roughly equal atomic percentages [13, 14]. The shape memory effect (SME) appears in some special alloys which show a crystallographically reversible [15, 16], thermoelastic [7, 15, 17] martensitic

Corresponding author : shangasepaul@gmail.com

transformation with the ability to recover large strains after plastic deformation, only by a change of temperature (one-way effect) [16-19].

Although, shape memory alloys have attractive properties for various applications there is a limit to their functional properties such as super-elasticity and shape memory effect, they cannot perform well above 100°C [19, 20]. Thus, there is a need to improve these functional properties of these alloys for high temperature applications, by an introduction of ternary alloying elements namely Au, Hf, Pd, Pt and Zr to the NiTi system to produce alloys with transformation temperatures exceeding 100°C [20]. Research indicates that the majority of alloying elements reduce transition temperatures, while only a select few, such as Hf, Zr, Pd, Pt, and Au, elevate these temperatures [21]. Zirconium (Zr) has two advantages over other elements. Firstly, it is more economical than Au, Pd, Pt, and Hf [22]. Secondly, the incorporation of Zr into a binary NiTi results in greater weight reduction compared to other identified elements for the same molar fraction [23].

Alloying with Zr produces a high temperature shape memory (HTSMA) alloy which can be suitable for automotive and aerospace applications [7, 24, 25]. The casting method of producing NiTiZr parts is a simple inexpensive method to produce SMA. In addition, heat treatment of the cast metals is critical for customizing their characteristics to suit application needs. It uses controlled heating and cooling cycles to change the microstructure, leading to increased strength, hardness and ductility while maintaining their shape memory properties.The aim of this study is to examine the influence of heat treatment temperatures and duration on the microstructural evolution and mechanical properties of $Ni_{50}Ti_{30}Zr_{20}$ high temperature alloys.

## 2 Materials and methods

One kilogram of feedstock was created by blending commercially pure Ni (99.9%, 200 μm), Ti (99.9%, 0.9–45 μm), and Zr (99.9%, 0.9–45 μm) powders (LGC Standards, UK) in a 50:30:20 weight percent ratio. Using a Ti getter, 20 grams of the mixture were arc-melted under argon in a water-cooled copper crucible to create metallic buttons that were divided into specimens measuring 5 × 10 × 10 mm. After three hours of argon solution treatment at 1000 °C, all samples were quenched with water. For one to three hours, aging was carried out at 550 °C, 750 °C, and 800 °C to examine precipitation behaviour and high-temperature reaction. A JEOL JSM-7600F SEM with Oxford EDS was used to perform microstructural investigation on polished cross-sections that had been produced by resin mounting, grinding, and diamond polishing. Three sites per sample underwent Vickers microhardness testing (Zwick Roell ZHμ, 10 g load, 20 s dwell), and mean values were noted.

### 2.1 Materials

One kilogram of powder was created by blending individual powders of 99.9% Ni (average particle size: 200 μm), 99.9% Ti (0.9–45 μm), and 99.9% Zr (0.9–45 μm) in mass proportions of 50% Ni, 30% Ti, and 20% Zr by mass. Commercially pure powders supplied by LGC Standards (UK) were used.

### 2.2 Methods

A total of 20 g of powder was measured for casting. The casting process was carried out using a button arc furnace equipped with a copper hearth and a water-cooled, commercially pure copper crucible, which facilitated easy removal of the solidified sample after cooling. Prior

to melting, the furnace chamber was purged three times with argon to minimise contamination. A titanium button was placed inside the chamber to act as an oxygen scavenger during the process. The powder was melted in the crucible under an inert argon atmosphere to ensure high purity of the final cast sample. The resulted melt was in the form of a metal NiTiZr button. The button was cut into six samples of 5 × 10 × 10 mm in size.

### *2.2.1 Heat treatments*

Heat treatments were performed to study the effects of microstructural changes and subsequent mechanical properties. These heat treatments were performed in a vertical tube furnace under an argon atmosphere. In order to remove the effects of casting and any inhomogeneity, solution treatment at a temperature of 1000°C for 3 hours was performed for each sample. This was followed by aging heat treatments to determine the effects of temperature on microstructural and mechanical properties. There were three aging heat treatment temperatures applied in this work, namely 550, 750 and 800°C. Aging at 550°C was chosen because it is generally the accepted peak aging temperature for Ni-rich NiTiZr high temperature shape memory alloys [19, 21]. Aging at 750°C was chosen because it was expected to increase the rate of precipitation and the number of precipitates and therefore, increase the material's strength. Aging at 800°C was chosen to investigate the material's response to high temperature applications. The time period for aging ranged from 1 hour to 3 hours. All samples were water quenched after each heat treatment.

### *2.2.2 Scanning electron microscopy*

The scanning electron microscopy, SEM JEOL JSM-7600F (JEOL, Akishima, Japan) equipped with an energy dispersive spectrometer (EDS) Inca Energy 350 SDD X-Max 20 mm2 (Oxford Instruments, Oxford, UK), was used for X-ray microanalysis. Samples were prepared by placing a small number of particles on conductive carbon tape that was fastened to a specimen mount. Loose debris on the mount was removed using pressurized air. Secondary electron imaging (SEI) mode was used to analyse the morphology and particle size of the powder blend. The powder samples were also mounted in a carbon resin, successively ground to a 15 μm finish and then polished with diamond polishing paste on a Struers MD-Chem (Germany) pad for 7 min. Exposed polished section surfaces of the powder particles were examined by EDS to determine contamination, phase evolution, alloying degree, and chemical homogeneity.

### *2.2.3 Vickers hardness testing*

A Vickers microhardness tester, model ZHμ, manufactured by Zwick Roell GmbH & Co. KG, located in Ulm, Germany was used for measuring microhardness. Measurements were conducted with a 10g load for 20 second durations on mounted, ground, and polished cross-sections of the samples. A diamond indenter was used for the indentation, and a 400 × microscopic lens attached to a Vickers tester was used to scan the indented area. Each sectioned sample was subjected to three distinct microhardness measures (side, middle, and center), and the sample surface was indented. Three indentations were averaged to provide the representative hardness value at each location.

## 3 Results

### 3.1 Powder characterisation

The EDS-SEM analysis confirmed the elemental powder composition. Figure 1 shows that the ball-milled blend has achieved near-target composition with reasonably good elemental distribution. Nickel and zirconium are well dispersed, while titanium still shows some segregation Additionally, a PSD analysis was performed on the blended powder. The particle shapes of the blended powder varied from irregular to globular, with an average size of 35.08 µm, Figure 2.. Ni and Zr show fairly uniform distribution, indicating significant progress toward homogeneity.

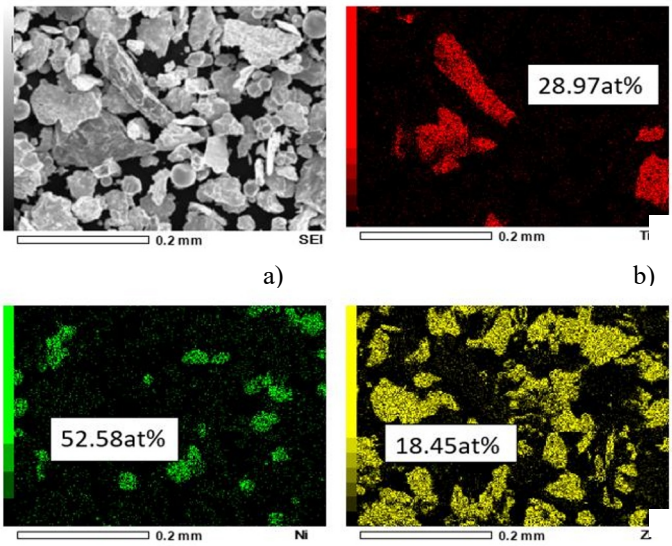


**Fig. 1.** Elemental mapping of the blended powder a), b), c) and d)

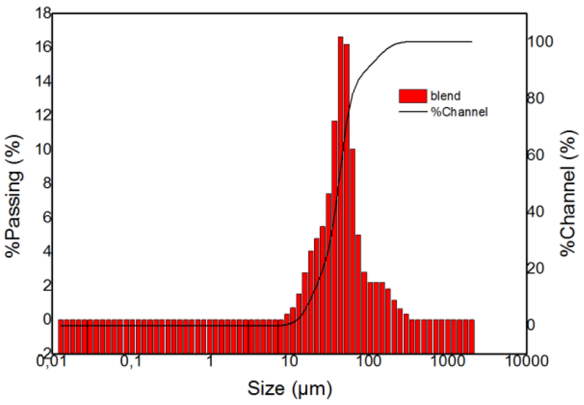


| Sizes | Blend (µm) |
|---|---|
| D10 | 18.93 |
| D50 | 41.71 |
| D90 | 92.09 |

**Fig. 2.** Particle size distribution of the blended powder

### 3.2 Microstructural characterisation

#### *3.2.1 As cast microstructures*

The as-cast micrograph of the $Ni_{50}Ti_{30}Zr_{20}$ alloy is displayed in Figure 3. The microstructure shows a dendritic structure and contains the phase B2. The grain shape was irregular. The point EDS of spectra displayed a consistent display of Ni, Ti and Zr in the sample (figure 3 and 4.

a)

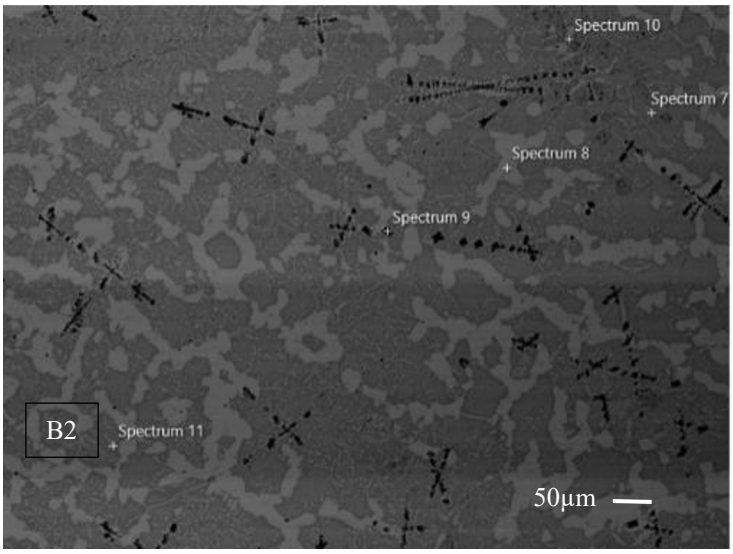


b)

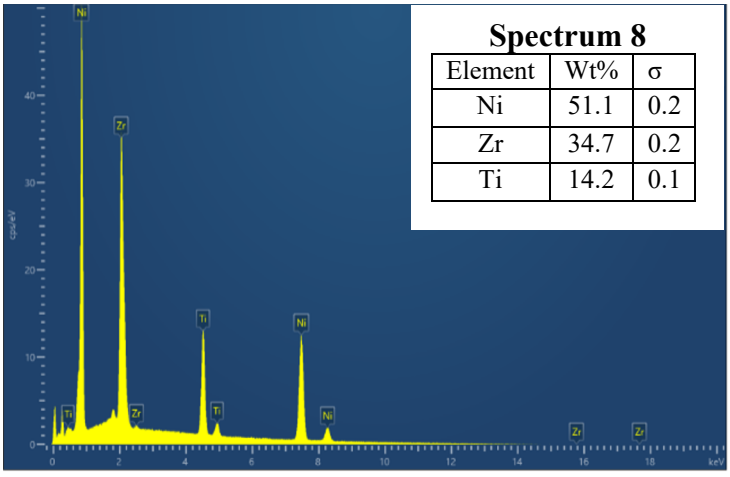


**Fig. 3.** As cast microstructure of NiTiZr a) SEM image and b) EDS of spectrum 8 position

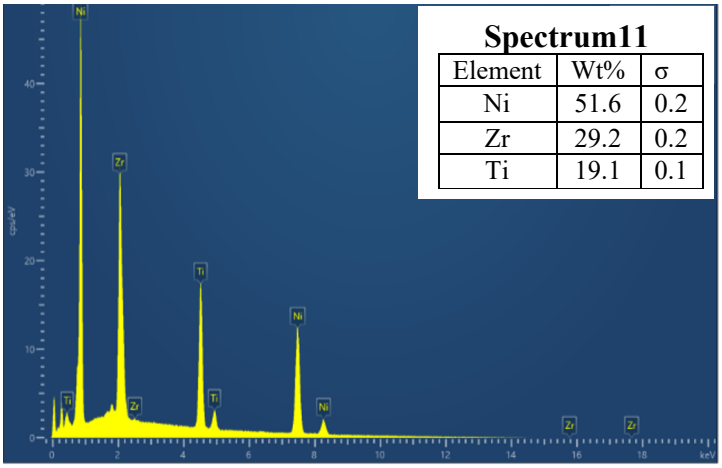


**Fig. 4**: EDS spectrum 11 position

### *3.2.2 Microstructures of heat-treated samples*

The images obtained from SEM display particles that are dispersedly distributed in the $Ni_{50}Ti_{30}Zr_{20}$ matrix in all the heat-treated samples 550, 750 and 800ºC. The time was varied from 1 to 3 hours. For the sample heat treated at 550ºC/1 h, there were less precipitates in the sample. The precipitates on the grain boundaries increased as the temperature increased from 550 to 750ºC, Figure 5(c). These results are consistent with what Smith et al [26] and Evirgen et al [27] found. dark contrast phase observed in the insertion of Figure 5a was identified as titanium oxide. The energy-dispersive x-ray spectroscopy (EDS) was employed to determine the composition of the oxides present in the microstructure and were found to be Ti-rich oxides with a composition of 53.3Ti – 1.56Zr – 0.6Ni – 44.6O at.%. The Ni might have been from the matrix. Grain size increased progressively with both aging temperature and duration, attaining a maximum value of 31 ±1.21µm following aging at 800 °C/3h, Figure 5.

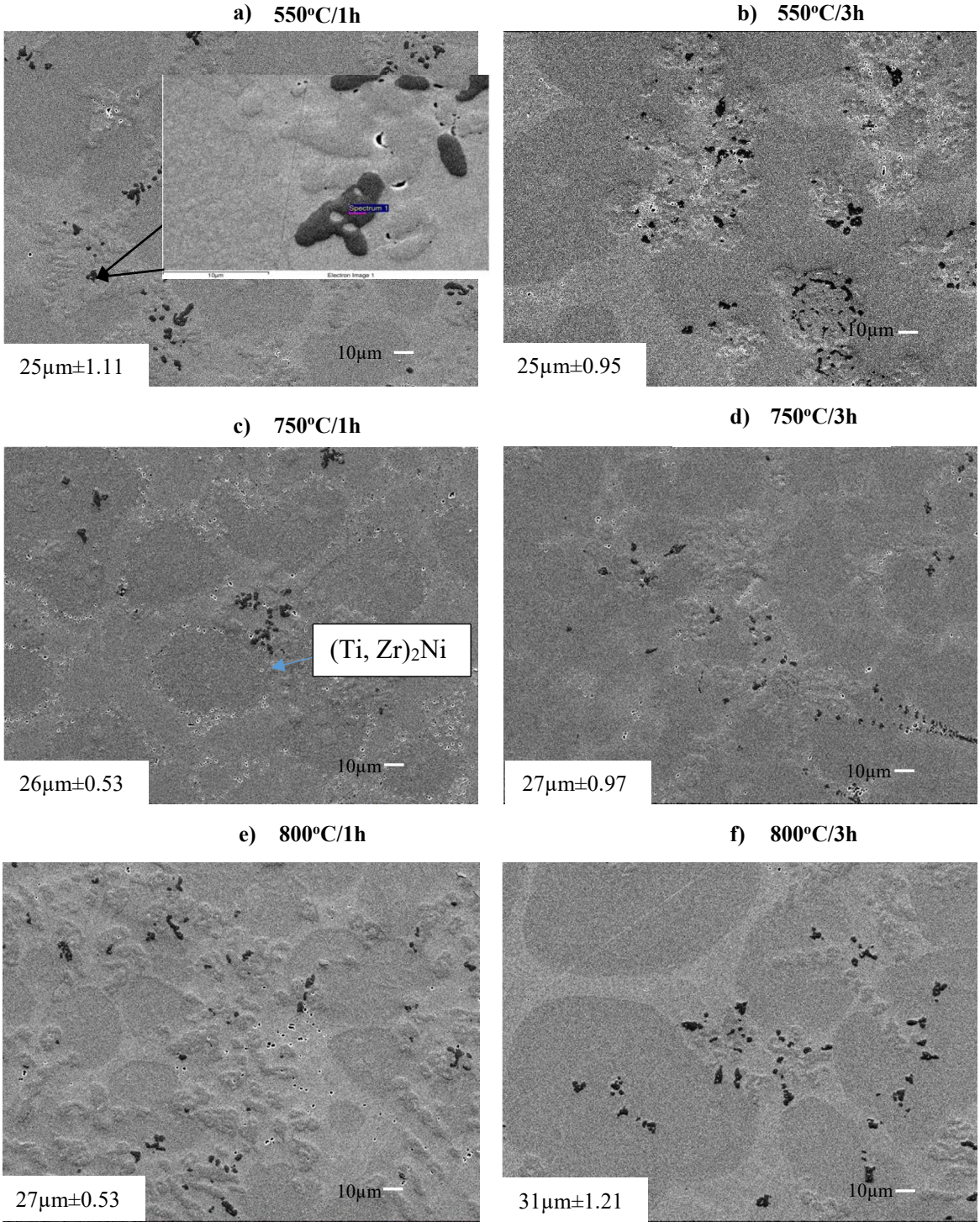


**Fig. 5.** SEM micrographs of heat-treated samples at 550,750 and 800°C for 1 and 3 hours (Mag:500x)

### 3.3 X-Ray diffraction

The x-ray diffractograms of the cast samples are displayed in Figure 6. It was observed that there was a formation of new phases with the main ones being austenite B2 and martensite B'19 NiTi. The martensite B'19 and austenite B2 were in the position of maximum diffraction intensity which occurred at 2θ values of 44,5º and 48,7º. According to Smith et al [18], the NiTi phase can retain the B2 structure also for substitution of Ti by Zr up to 40%. It is plausible to define the B2 NiTi as Ni (Ti, Zr), where some of the Ti sites may be occupied by Zr atoms. In addition, there are weak diffraction peaks, which can be identified as NiTiZr, $NiTi_2$ and $Ni_3Ti$ phases. The dominant phase was determined to be a mixture of $(Ti, Zr)_2Ni$ co-existing with the matrix NiTiZr and B2 NiTi phases. The precipitate was identified to be $(Ti, Zr)_2Ni$ and was predominantly found on the grain boundaries of the 750ºC/1h sample's microstructure.

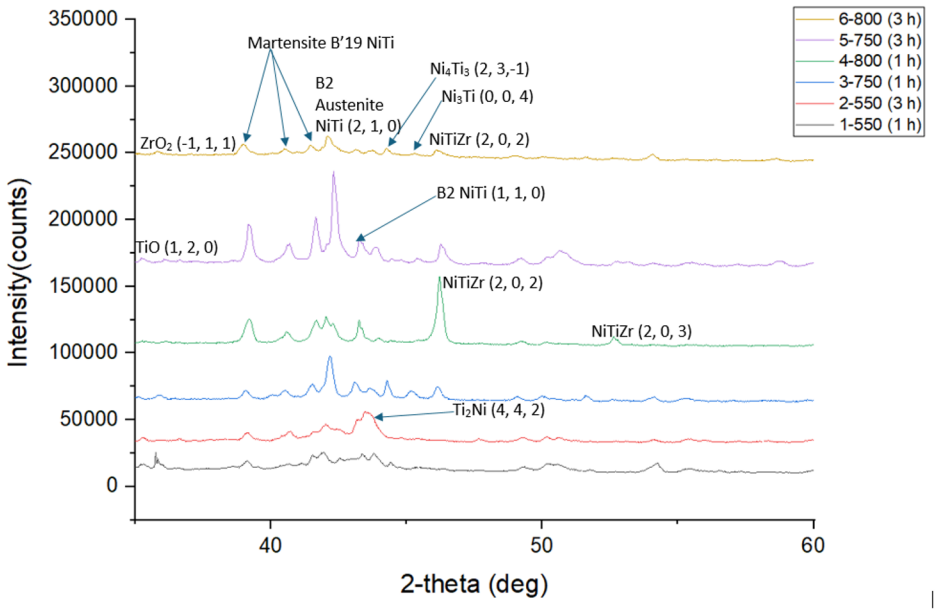


**Fig. 5.** X-ray diffractograms of the heat-treated samples

### 3.4 Vickers microhardness

Vickers hardness testing was employed as an initial assessment of the effect of the various heat treatments on the mechanical properties [8, 53]. Figure 7 presents the variations in Vickers hardness under different heat treatment conditions. The highest hardness value of 780 HV was observed in the sample aged at 750°C/3 h. Since high hardness generally leads to improved degradation resistance in NiTiZr alloys, the 750 °C/3 h aging condition was identified as the optimal treatment following solution annealing. Notably, increasing the aging temperature-time from 550 °C/1 h to 750 °C/3 h led to a significant increase in hardness

Corresponding author : shangasepaul@gmail.com

from 619 HV to 717 HV**.** However, increasing further the thermal exposure resulted in a decrease in hardness to 643 HV, indicating the onset of over-aging.

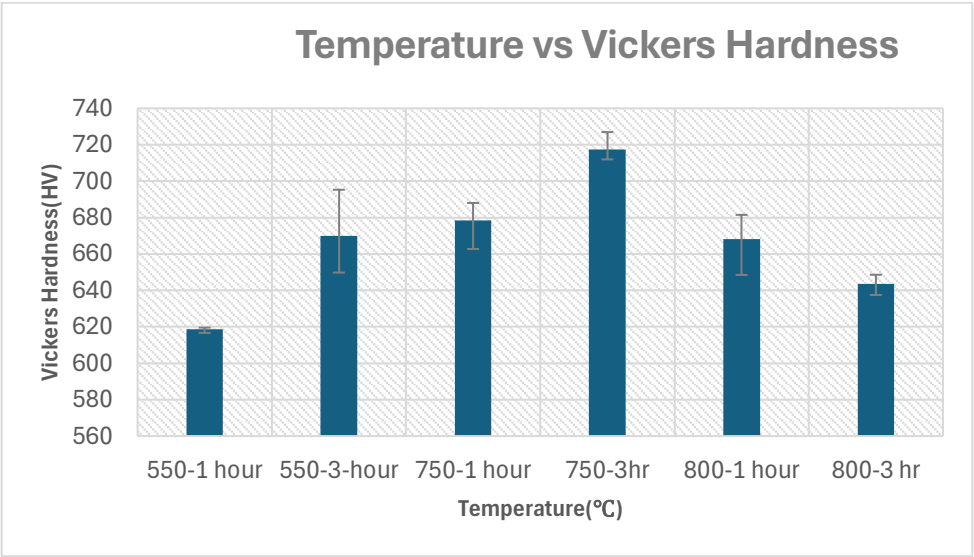


**Fig. 7.** Vickers hardness vs temperature-time for aged samples from 550℃/1h to 800℃/3h

## 4 Conclusions

The effect of heat treatment on the microstructural changes and properties of cast $Ni_{50}Ti_{30}Zr_{20}$ alloy was investigated and the following conclusions can be made:

- The study demonstrates that $Ni_{50}Ti_{30}Zr_{20}$ alloys can have their precipitation and hardness optimised through controlled aging at intermediate temperatures. This allows for customized microstructures for enhanced high-temperature shape memory performance while preventing the negative consequences of over-aging.
- Sample heat treated at 550ºC for 1 hour showed less precipitates on the grain boundaries. The grain boundaries precipitates increased as the temperature increased from 550 to 750ºC.
- Increasing the aging temperature-time from 550 °C/1 h to 750 °C/3 h led to a significant increase in hardness from 619 HV to 717 HV. However, increasing further the thermal exposure resulted in a slight decrease in hardness to 703 HV, indicating the onset of over-aging.

The development of lightweight smart materials for energy-efficient designs is encouraged by this work, which lessens the need for more costly, heavier alloying elements like Hf, Pd, or Pe. The adoption of NiTiZr alloys in actuators, connections, and morphing structures where greater operating temperatures are needed is also made possible by this.

## References

[1] N. Sharma, T. Raj, and K. K. Jangra, Microstructural evaluation of NiTi-powder, steatite, and steel balls after different milling conditions, Mat. and Man. Proc., vol. 31, no. 5, pp. 628-632, 2016. https://doi.org/10.1080/10426914.2015.1004710

[2] M. E. Mondejar *et al.*, Digitalization to achieve sustainable development goals: Steps towards a Smart Green Planet, Sci. of The Tot. Envi., vol. 794, p. 148539, 2021. https://doi.org/10.1016/j.scitotenv.2021.148539

[3] P. J. Wellmann, The search for new materials and the role of novel processing routes, Dis. Mat., vol. 1, no. 1, p. 14, 2021. https://doi.org/10.1007/s43939-021-00014-y

[4] F. Butera, Shape Memory Alloys, Adv. Mat. & Proc., vol. 166, no. 3, 2008.

[5] D. Stoeckel, Shape memory actuators for automotive applications, Mat. & Des., vol. 11, no. 6, pp. 302-307, 1990. https://doi.org/10.1016/0261-3069(90)90013-A

[6] C. Bil, K. Massey, and E. J. Abdullah, Wing morphing control with shape memory alloy actuators, J. of Int. Mat. Sys. and Struc., vol. 24, no. 7, pp. 879-898, 2013. https://doi.org/10.1177/1045389X12471866

[7] J. Van Humbeeck, High temperature shape memory alloys, 1999. https://doi.org/10.1115/1.2816006

[8] S. Dilibal, The Effect of Long-Term Heat Treatment on the Thermomechanical Behavior of NiTi Shape Memory Alloys in Defense and Aerospace Applications, J. of Def. Sci./Sav. Bil. Der., vol. 15, no. 2, 2016.

[9] M. Es-Souni, M. Es-Souni, and H. Fischer-Brandies, Assessing the biocompatibility of NiTi shape memory alloys used for medical applications, An. and bio. chem., vol. 381, pp. 557-567, 2005.

[10] Y. Furuya and H. Shimada, Shape memory actuators for robotic applications, Mat. & Des., vol. 12, no. 1, pp. 21-28, 1991. https://doi.org/10.1016/0261-3069(91)90088-L

[11] S. K. Patel, B. Behera, B. Swain, R. Roshan, D. Sahoo, and A. Behera, A review on NiTi alloys for biomedical applications and their biocompatibility, Mat. tod.: proc., vol. 33, pp. 5548-5551, 2020. https://doi.org/10.1016/j.matpr.2020.03.538

[12] M. M. Lazić *et al.*, A brief overview and application of Nickel-Titanium shape memory alloy in dentistry, Tit.-Based Al.-Char and App., 2024. DOI: 10.5772/intechopen.1004825

[13] N. Sharma, T. Raj, and K. Jangra, Applications of nickel-titanium alloy, J. of Eng. and Tech., vol. 5, no. 1, p. 1, 2015. https://doi.org/10.1177/1464420715622494

[14] S. Takaoka, Overview of the development of shape memory and superelastic alloy applications, in Sh.Mem. and Super All: Elsevier, 2011, pp. 77-84. https://doi.org/10.1533/9780857092625.1.77

[15] C. Laureanda, One Way and Two Way—Shape Memory Effect: Thermo—Mechanical Characterization of Ni—Ti Wires, Universitá degli Studi di Pavia Pavia, Italy, 2008.

[16] A. Falvo, M. L. Luchi, and F. Fugiuele, Thermomechanical characterization of Nickel-Titanium shape memory alloys, 2007.

[17] J. Cui *et al.*, Combinatorial search of thermoelastic shape-memory alloys with extremely small hysteresis width, Nat. mat., vol. 5, no. 4, pp. 286-290, 2006.

[18] M. Carl, J. D. Smith, B. Van Doren, and M. L. Young, Effect of Ni-content on the transformation temperatures in NiTi-20 at.% Zr high temperature shape memory alloys, Met., vol. 7, no. 11, p. 511, 2017.

[19] A. N. Khan, M. Muhyuddin, and A. Wadood, Development and characterization of Nickel–Titanium–Zirconium shape memory alloy for engineering applications, Russ. J. of Non-Ferr. Met., vol. 58, pp. 509-515, 2017. DOI: 10.3103/S1067821217050078

[20] K. Otsuka and X. Ren, Physical metallurgy of Ti–Ni-based shape memory alloys, Prog. in mat. sci., vol. 50, no. 5, pp. 511-678, 2005. https://doi.org/10.1016/j.pmatsci.2004.10.001

[21] S. Hsieh and S. Wu, A study on ternary Ti-rich TiNiZr shape memory alloys, Mat. char., vol. 41, no. 4, pp. 151-162, 1998. https://doi.org/10.1016/S1044-5803(98)00032-1

[22] A. Evirgen, Microstructural characterization and shape memory response of Ni-rich NiTiHf and NiTiZr high temperature shape memory alloys, 2014.

[23] J. Ma, I. Karaman, and R. D. Noebe, High temperature shape memory alloys, Inter. Mat. Rev., vol. 55, no. 5, pp. 257-315, 2010. https://doi.org/10.1179/095066010X12646898728363

[24] G. Firstov, J. Van Humbeeck, and Y. N. Koval, High-temperature shape memory alloys: some recent developments, Mat. Sci. and Eng.: *A,* vol. 378, no. 1-2, pp. 2-10, 2004. https://doi.org/10.1016/j.msea.2003.10.324

[25] O. Karakoc *et al.*, Effects of training on the thermomechanical behavior of NiTiHf and NiTiZr high temperature shape memory alloys, Mat. Sci. and Eng.: *A,* vol. 794, p. 139857, 2020. https://doi.org/10.1016/j.msea.2020.139857

[26] M. A. Carl, Alloy development and high-energy X-ray diffraction studies of NiTiZr and NiTiHf high temperature shape memory alloys. 2018.

[27] A. Evirgen, J. Pons, I. Karaman, R. Santamarta, and R. Noebe, H-Phase precipitation and martensitic transformation in Ni-rich Ni–Ti–Hf and Ni–Ti-Zr high-temperature shape memory alloys, Sh. Mem. and Super., vol. 4, pp. 85-92, 2018.